Design of Polymeric Si−B−C−N Ceramic Precursors for Application in Fiber-Reinforced Composite Materials

Markus Weinmann,*,† Thomas W. Kamphowe,†,§ Jörg Schuhmacher,‡ Klaus Müller,‡ and Fritz Aldinger†

Max-Planck-Institut für Metallforschung and Institut für Nichtmetallische Anorganische Materialien, Universität Stuttgart, Pulvermetallurgisches Laboratorium, Heisenbergstrasse 5, 70569 Stuttgart, Germany, and Institut für Physikalische Chemie, Universität Stuttgart, Pfaffenwaldring 55, 70569 Stuttgart, Germany

Received March 8, 2000. Revised Manuscript Received May 5, 2000

The synthesis, detailed spectroscopic characterization, polymer-to-ceramic conversion, and high-temperature behavior of a new class of polymeric precursors for Si−B−C−N composites are discussed. The title compounds $[B(C_2H_4{-}SiR^1R^2{-}C_2H_4{-}SiHNH)_3]_n$ (C_2H_4 = $CHCH_3$, CH_2-CH_2; **5a**: R^1, R^2 = H; **5b**: R^1 = H, R^2 = CH_3; **5c**: R^1, R^2 = CH_3) were designed especially for the preparation of ceramic films and fiber-reinforced ceramic composite matrixes. They are obtained in quantitative yields by the reaction of oligovinylsilazane $[(H_2C{=}CH)SiH{-}NH]_n$ (**4**) with tris(hydridosilylethyl)boranes of general type $B(C_2H_4SiHR^1R^2)_3$ (C_2H_4 = $CHCH_3$, CH_2CH_2; **3a**: R^1, R^2 = H; **3b**: R^1 = H, R^2 = CH_3; **3c**: R^1, R^2 = CH_3) in a thermally induced hydrosilylation reaction without catalyst and/or solvent and without the formation of byproducts. Ceramic yields are 83% for **5a**, 82% for **5b**, and 63% for **5c** as shown by thermogravimetric analysis (TGA). High-temperature TGA of the as-obtained amorphous ceramic materials, carried out in an argon atmosphere, reveals a thermal stability toward degradation of the **5b**-derived material **6b** up to 2000 °C. In contrast, the **6a** material, which was obtained from **5a**, decomposes around 1850 °C. The least stable is the **6c** ceramic, which decomposes at 1450 °C. The microstructure development of **6a**−**6c** was investigated in the temperature range of 1400−2000 °C by X-ray diffraction (XRD), indicating that preferentially crystalline α-silicon carbide is formed at 1700 °C for **6a**, 1500 °C for **6b**, and 1600 °C for **6c**. In addition, there are less intensive reflections observed in the XRD patterns of **6a**, caused by the formation of β-silicon nitride.

1. Introduction

Choosing a material basis for high-temperature structure materials suffers from a principal dilemma. Oxide materials show creep affinity at high temperatures, limiting their application in energy facilities and the aerospace industry.[1] Non-oxide materials, which possess increased creep stability at high temperatures, are not thermodynamically stable in air and react with oxygen and/or moisture.[2] Those which form protective oxide layers either contain oxide-type grain boundary phases promoting creep and increased internal oxygen diffusion at higher temperatures or have lower toughness values. Promising candidates for high-temperature oxidation resistance are those covalent ceramics that are prepared without sintering additives. These materials are usually obtained by thermolysis of suitable organometallic polymers (=precursors) in an inert gas atmosphere.[3−8] Because of low self-diffusion coefficients in covalent ceramics, conventional sintering of powder compacts without additives is not suitable for the production of composites based on covalent ceramics.[9] Multinary non-oxide ceramics are of special interest because these materials combine properties of the constituting binary phases. In this context amorphous Si−B−C−N ceramics obtained from organosilicon precursors became of fundamental interest because these materials recently demonstrated a short-time thermal stability up to 2000 °C without mass loss and/or crystallization.[10−12] This

* To whom correspondence should be addressed. E-mail: weinmann@aldix.mpi-stuttgart.mpg.de.
† Max-Planck-Institüt für Metalforchung, Stuttgart.
‡ Institut für Physikalische Chemie, Universität Stuttgart.
§ Present address: Sethweg 65, 22455 Hamburg, Germany.

(1) Evans, A. G. Ceramic and Ceramic Composites as High-temperature Structural Materials: Challenges and Opportunities. In *High-Temperature Structural Materials*; Cahn, R. W., Evans, A. G., McLean, M., Eds.; Chapman & Hall: London, 1996.
(2) See for example: (a) Gogotsi, Y. G.; Lavrenko, V. A. *Corrosion of High-Performance Ceramics*; Springer- Verlag: Berlin, 1992. (b) Jorgensen, P. J.; Wadsworth, M. E.; Cutler, I. B. *J. Am. Ceram. Soc.* **1959**, *42*, 613. (c) Franz, I.; Langheinrich, W. *Solid State Electron.* **1971**, *14*, 499.
(3) Peuckert, M.; Vaahs, T.; Brück, M. *Adv. Mater.* **1990**, *2*, 398.
(4) Toreki, W. *Polym. News* **1991**, *16*, 1.
(5) Birot, M.; Pillot, J.-P.; Dunogués, J. *Chem. Rev.* **1995**, *95*, 1443.
(6) Bill, J.; Aldinger, F. *Adv. Mater.* **1995**, *7*, 775.
(7) Riedel, R. Advanced Ceramics from Inorganic Polymers. In *Materials Science and Technology*; Cahn, R. W., Haasen, P., Kramer, E. J., Eds.; VCH: Weinheim, 1996; Chapter 11, p 1.
(8) Baldus, H.-P.; Jansen, M. *Angew. Chem.* **1997**, *109*, 338; *Angew. Chem., Int. Ed. Engl.* **1997**, *36*, 328.
(9) (a) Kleebe, H.-J. *J. Ceram. Soc. Jpn.* **1997**, *105*, 453, and literature cited therein. (b) Lewis, M. H.; Leng-Ward, G.; Mason, S. *Br. Ceram. Proc.* **1987**, *39*, 1.
(10) Baldus, H.-P.; Jansen, M.; Wagner, O. *Key Eng. Mater.* **1994**, *89−91*, 75.
(11) Riedel, R.; Kienzle, A.; Dressler, W.; Ruwisch, L. M.; Bill, J.; Aldinger, F. *Nature* **1996**, *382*, 796.

10.1021/cm001031w CCC: $19.00
Published on Web 07/14/2000

attribute, coupled with a high resistance toward oxidative attack at elevated temperatures,[12] gives rise to extensive studies.

Takamizawa et al. in 1986 reported, for the first time, on the high-temperature stability of Si−B−C−N composites.[13] Soon after, Seyferth and co-workers described the synthesis of silazane-substituted borazine as a Si−B−C−N precursor, which was obtained by the reaction of borane dimethyl sulfide and cyclotrisilazane.[14] Si−B−C−N preceramics that are also based on borazine were obtained by Sneddon and co-workers by dehydrogenation and dehydrosilylation of hydridosilazanes with borazine.[15] Recent publications of Srivastava et al. describe an interesting method for the synthesis of borazine-based Si−B−C−N precursors using B-chloroborazines as starting compounds.[16] In 1992, Baldus and co-workers described the synthesis of poly(*N*-methylborosilazane), obtained by aminolysis of $Cl_3SiNHBCl_2$ (TADB).[10,17] At the same time Riedel and co-workers obtained Si−B−C−N precursors by ammonolysis of tris(methyldichlorosilylethyl)borane.[18] In both cases, the obtained ceramics possess outstanding thermal stability, as was determined by X-ray diffraction (XRD)[8,10] and thermogravimetric analysis (TGA).[11] Recently, we developed a synthetic process for the synthesis of highly cross-linked Si−B−C−N precursors by a non-oxide sol−gel process.[19] Highly cross-linked polysilylcarbodiimides were obtained from $B[C_2H_4-Si(R)Cl_2]_3$ (R = H, Cl, CH_3) and bis(trimethylsilyl)carbodiimide. In a *trans*-silylation reaction, C−B−C cross-linked [−Si(R)−N=C=N−] polymer frameworks were built.

All the above-described polymeric precursors are synthesized in solution with the formation of byproducts. Both features limit the applicability of these systems for advanced technologies, for example, the preparation of fiber-reinforced ceramic composites. In contrast to polymer matrix composites based on polyester or epoxy resins, there is to our knowledge no resin in the Si−B−C−N system known so far, which allows similar techniques for the production of fiber-reinforced Si−B−C−N ceramics.

It is the purpose of this paper to describe the initial results of the development of novel Si−B−C−N preceramic polymers by a thermally induced hydrosilylation reaction, particularly considering the aspects mentioned above. In contrast to established procedures, the formation of highly cross-linked Si−B−C−N polymers occurs by a polyaddition reaction of oligovinylsilazane, $[H_2C{=}CH)SiHNH]_n$,[20] and tris(hydridosilylethyl)boranes of general structure $B[C_2H_4-Si(CH_3)_nH_{3-n}]_3$ (n = 0 − 2)[21] without the use of solvents or catalysts and, more importantly, without the production of byproducts.

2. Experimental Section

2.1. General Comments. All reactions were carried out in a purified argon atmosphere using standard Schlenk techniques.[22] The synthesis of oligovinylsilazane (OVS, **4**), $[(H_2C{=}CH)SiHNH]_n$, was performed according to the procedures described in the literature by Choong Kwet Yive and coworkers.[20] Tris(hydridosilylethyl)boranes, $B[C_2H_4-Si(CH_3)_nH_{3-n}]_3$ (**3a**−**c**, n = 0 − 2), were obtained according to ref 21.

Fourier-infrared spectra were obtained with a Bruker IFS66 spectrometer in a KBr matrix. Solid-state NMR experiments were performed on a Bruker CXP 300 or a Bruker MSL 300 spectrometer operating at a static magnetic field of 7.05 T (^{1}H frequency: 300.13 MHz) using a 4-mm magic angle spinning (MAS) probe. ^{29}Si and ^{13}C NMR spectra were recorded at 59.60 and 75.47 MHz using the cross-polarization (CP) technique in which a spin lock field of 62.5 kHz and a contact time of 3 ms were applied. Typical recycle delays were 6−8 s. All spectra were acquired using the MAS technique with a sample rotation frequency of 5 kHz. ^{29}Si and ^{13}C chemical shifts were determined relative to external standard Q_8M_8, the trimethylsilylester of octameric silicate and adamantane, respectively. These values were then expressed relative to the reference compound TMS (0 ppm). High-resolution ^{1}H NMR spectra of tris(hydridosilylethyl)boranes were recorded on a Bruker ARX500 spectrometer (nominal frequency: 500.133 MHz). Elemental analysis was performed using different apparatuses (Elementar, Vario EL CHN− Determinator; ELTRA, CS 800, C/S Determinator; LECO, TC-436, N/O Determinator) and by atom emission spectrometry (ISA JOBIN YVON JY70 Plus). TGA of the polymer-to-ceramic conversion was carried out in a flowing argon atmosphere (50 cm^3/min) with a Netzsch STA 409 in alumina crucibles over a temperature range of 25−1400 °C (heating rate: 2 °C/min). Bulk ceramization of preceramic material occurred in alumina Schlenk tubes in flowing argon at 25−1400 °C, heating rate of 1 °C/min, and a dwell time of 3 h. A Netzsch STA 501 was used for the high-temperature TGA of the as-obtained ceramic samples in an argon atmosphere over a temperature range of 25−2200 °C (heating

(12) Weinmann, M.; Schuhmacher, J.; Kummer, H.; Prinz, S.; Peng, J.; Seifert, H. J.; Christ, M.; Müller, K.; Bill, J.; Aldinger, F. *Chem. Mater.* **2000**, *12*, 623.

(13) Takamizawa, M.; Kobayashi, T.; Hayashida, A.; Takeda, Y. U.S. Patent 4,604,367, 1986.

(14) (a) Seyferth, D.; Plenio, H. *J. Am. Ceram. Soc.* **1990**, *73*, 2131. (b) Seyferth, D.; Plenio, H.; Rees, W. S., Jr.; Büchner, K. In *Frontiers of Organosilicon Chemistry*; Bassindale, A. R., Gaspar, P. P., Eds.; Royal Society of Chemistry: Cambridge, 1991; p 15.

(15) (a) Su, K.; Remsen, E. E.; Zank, G. A.; Sneddon, L. G. *Chem. Mater.* **1993**, *5*, 547. (b) Su, K.; Remsen, E. E.; Zank, G. A.; Sneddon, L. G. *Polym. Prepr. (Am. Chem. Soc., Div. Polym. Chem.)* **1993**, *34*, 334. (c) Wideman, T.; Su, K.; Remsen, E. E.; Zank, G. A.; Sneddon, L. G. *Chem. Mater.* **1995**, *7*, 2203. (d) Fazon, P. J.; Remsen, E. E.; Beck, J. S.; Carroll, P. J.; McGhie, A. R.; Sneddon, L. G. *Chem. Mater.* **1995**, *7*, 1942. (e) Wideman, T.; Su, K.; Remsen, E. E.; Zank, G. A.; Sneddon, L. G. *Mater. Res. Soc. Symp. Proc.* **1996**, *410*, 185. (f) Wideman, T. T.; Cortez, E.; Remsen, E. E.; Zank, G. A.; Carroll, P. J.; Sneddon, L. G. *Chem. Mater.* **1997**, *9*, 2218.

(16) Srivastava, D.; Duesler, E. N.; Paine, R. T. *Eur. J. Inorg. Chem.* **1998**, 855.

(17) (a) Jansen, M.; Baldus, H.-P. Ger. Offen. DE 410 71 08 A1, 1992. (b) Baldus, H.-P.; Wagner, O.; Jansen, M. *Mater. Res. Soc. Symp. Proc.* **1992**, *271*, 821. (c) Jansen, M. *Solid State Ionics* **1998**, *101*−*103*, 1.

(18) (a) Kienzle, A. Diploma Thesis, Univeristät Stuttgart, Germany, 1991 (in German). (b) Kienzle, A. Ph.D. Thesis, Universität Stuttgart, Germany, 1994 (in German). (c) Riedel, R.; Kienzle, A.; Petzow, G.; Brück, M.; Vaahs, T. Ger. Offen. DE 432 07 83 A1, 1994. (d) Riedel, R.; Kienzle, A.; Petzow, G.; Brück, M.; Vaahs, T. Ger. Offen. DE 432 07 84 A1, 1994. (e) Bill, J.; Kienzle, A.; Sasaki, M.; Riedel, R.; Aldinger, F. In *Ceramics: Charting the Future*; Vincenzini, P., Ed.; Techna Srl, 1995.

(19) (a) Weinmann, M.; Haug, R.; Bill, J.; Aldinger, F.; Schuhmacher J.; Müller, K. *J. Organomet. Chem.* **1997**, *541*, 345. (b) Weinmann, M.; Haug, R.; Bill, J.; De Guire, M.; Aldinger, F. *Appl. Organomet. Chem.* **1998**, *12*, 725. (c) Haug, R.; Weinmann, M.; Bill, J.; Aldinger, F. *J. Eur. Ceram. Soc.* **1999**, *19*, 1.

(20) (a) Lavedrine, A.; Bahloul, D.; Goursat, P.; Choong Kwet Yive, N. S.; Corriu, R. J.; Leclercq, D.; Mutin, P. H.; Vioux, A. *J. Eur. Ceram. Soc.* **1991**, *8*, 221. (b) Choong Kwet Yive, N. S.; Corriu, R. J.; Leclercq, D.; Mutin, P. H.; Vioux, A. *New J. Chem.* **1991**, *15*, 85. (c) Choong Kwet Yive, N. S.; Corriu, R. J.; Leclercq, D.; Mutin, P. H.; Vioux, A. *Chem. Mater.* **1992**, *4*, 141. (d) Bahloul, D.; Pereira, M.; Goursat, P.; Choong Kwet Yive, N. S.; Corriu, R. J. *J. Am. Ceram. Soc.* **1993**, *76*, 1156.

(21) (a) Kamphowe, T. W. Ph.D. Thesis, Universität Stuttgart, Germany, 1999 (in German). (b) Weinmann, M.; Bill, J.; Aldinger, F. Ger. Offen. DE 197 41 459 A1, 1999. (c) Weinmann, M.; Kamphowe, T. W.; Fischer, F.; Aldinger, F. *J. Organomet. Chem.* **1999**, *592*, 115.

(22) This preparative method is based on experiments developed by the German chemist Wilhelm Schlenk. All apparatus are equipped with side arms for pumping out the air and moisture and introducing inert gas. See also: Shriver, D. F.; Drezdzon, M. A. *The Manipulation of Air-Sensitive Compounds*, 2nd ed.; Wiley: New York, 1986.

rate: T < 1400 °C, 5 °C/min; T > 1400 °C, 2 °C/min) using carbon crucibles. High-temperature TGA in air (25−1700 °C; heating rate: 5 °C/min) was performed using alumina crucibles. The crystallization of as-obtained amorphous ceramics was investigated in graphite furnaces using graphite crucibles at 1400 and 1500−2000 °C in 50 °C steps (heating rate: T < 1400 °C, 10 °C/min; T > 1400 °C, 2 °C/min). The X-ray diffraction unit used for the structural investigations of the annealed samples was a Siemens D5000/Kristalloflex with Cu $K\alpha_1$ radiation, equipped with an OED and a quartz primary monochromator. Scanning electron microscopy investigations were performed with ZEISS DSM982 Gemini field emission equipment equipped with a Schottky field emitter. RTM (resin transfer molding) was performed using the vacuum injection method in equipment designed especially for air-sensitive compounds (Figure 10). The brass mold was Teflon-sprayed to avoid adhesion of the precursor. Torayca carbon woven fabrics were used without initial treatment.

2.2. Polymer Synthesis and Characterization. In a typical experiment 30 mmol (2.13 g) of $[(H_2C{=}CH)SiH{-}NH]_n$ (**4**) and 10 mmol of $B[C_2H_4{-}Si(CH_3)_nH_{3-n}]_3$ (**3a**, $n = 0$: 1.88 g; **3b**, $n = 1$: 2.30 g; **3c**, $n = 2$: 2.73 g) were mixed in a Schlenk tube at room temperature. Under vigorous magnetic stirring, the mixture was evacuated two times until a foaming due to dissolved gas stopped and then it was slowly saturated with argon. Next, the Schlenk tube was heated to 120 °C within 2 h. The reaction mixtures, which increased in viscosity with increasing temperature, were finally heated to 200 °C (heating rate: 120−200 °C, 20 °C/h approximately) to form the transparent glasslike polymers.

2.2.1. $[B(C_2H_4SiH_2C_2H_4SiHNH)_3]_n$ (5a). Anal. Found: C, 31.4; H, 9.2; N, 13.3; B, 2.5; Si, 43.6. $[C_{12}H_{36}N_3BSi_6]_n$ ($[401.76]$)$_n$. Calcd: C, 35.9; H, 9.0; N, 10.5; B, 2.7; Si, 41.9. IR (KBr): ν (N−H) = 3440 vbr, 3403 vbr; ν (C−H) = 2965 m, 2921 m; ν (Si−H) = 2144 vs; δ (CH_2, bending) = 1457 m; δ_{as} (CH_3) = 1403 m; δ_s (C−C) = 1384 s; ν (C−C) = 1162 m; ν_{as} (C−B−C) = 1076 s cm^{-1}. ^{1}H MAS NMR: δ = 1.0 vbr (N*H*, var. C*H*), 3.5−4.5 vbr (C_2SiH_2, N_2SiH). ^{13}C CP-MAS NMR: δ = 14.0 (SiCH_2, CHCH_3), 27.0 sh, br (*C*H, *C*H_2). ^{29}Si CP-MAS NMR: δ = −31.9 ($H_2SiC(sp^3)_2$), −20.0 ($HSiN_2C(sp^3)$). TGA (1400 °C, 83% ceramic yield): 25−300 °C, Δm = 6%; 450−650 °C, Δm = 9%; 650−1400 °C, Δm = 2%.

2.2.2. $[B(C_2H_4SiH(CH_3)C_2H_4SiHNH)_3]_n$ (5b). Anal. Found: C, 39.1; H, 8.8; N, 10.6; B, 2.2; Si, 39.3. $[C_{15}H_{42}N_3BSi_6]_n$ ($[443.84]$)$_n$. Calcd: C, 40.6; H, 9.5; N, 9.5; B, 2.4; Si, 38.0. IR (KBr): ν (N−H) = 3423 br; ν (C−H) = 2956 m, 2917 m, 2869 m; ν (Si−H) = 2129 vs; δ (CH_2, bending) = 1457 m; δ_{as} (CH_3) = 1405 m; δ_s (C−C) = 1384 m; δ (C−H) = 1309 m; δ_s (Si−C) = 1253 m; ν (C−C) = 1166 m; δ (CH_3, rocking) = 948 s; γ (Si−H, wagging) = 887 vs cm^{-1}. ^{1}H MAS NMR: δ = −0.1 (SiCH_3), 0.8 (N*H*, var. C*H*), 3.6 (C_3SiH), 4.5 (N_2SiH). ^{13}C CP-MAS NMR: δ = −6.5 (SiCH_3), 13.5 (SiCH_2, CHCH_3), 24.0 br (*C*H, *C*H_2). ^{29}Si CP-MAS NMR: δ = −31.4 ($H_2SiC(sp^3)_2$), −18.0 ($HSiN_2C(sp^3)$), −11.5 ($HSiC_3(sp^3)$). TGA (1400 °C, 82% ceramic yield): 25−300 °C, Δm = 6%; 450−900 °C, Δm = 11%; 900−1400 °C, Δm = 1%.

2.2.3. $[B(C_2H_4Si(CH_3)_2C_2H_4SiHNH)_3]_n$ (5c). Anal. Found: C, 43.8; H, 9.4; N, 11.4; B, 2.2; Si, 33.2. $[C_{18}H_{48}N_3BSi_6]_n$ ($[485.92]$)$_n$. Calcd: C, 44.5; H, 10.0; N, 8.6; B, 2.2; Si, 34.7. IR (KBr): ν (N−H) = 3410 br; ν (=C−H) = 3054 w; ν (C−H) = 2956 m, 2906 m, 2869 m; ν (Si−H) = 2111 vs; δ (CH_2, bending) = 1457 w; δ_{as} (CH_3) = 1403 m; δ_s (C−C) = 1384 m; δ (C−H) = 1307 m; δ_s (Si−C) = 1249 s; ν (C−C) = 1168 s; γ (Si−H, wagging) = 883 vs; δ (Si−C, rocking) = 763 m cm^{-1}. ^{1}H MAS NMR: δ = −0.1 (SiCH_3), 0.9 (N*H*, var. C*H*), 3.8 (C_3SiH), 4.6 br (N_2SiH), 5.8 br (=C*H*). ^{13}C CP-MAS NMR: δ = −3.5 (SiCH_3), 1.2 (SiCH_3), 9.8 (SiCH_2, CHCH_3), 21.2 br (*C*H, *C*H_2), 133.0 br (=*C*H), 139.0 br (=*C*H). ^{29}Si CP-MAS NMR: δ = −34.8 ($HSiN_2C(sp^2)$), −21.4 ($HSiN_2C(sp^3)$), −11.9 ($HSiC_3(sp^3)$), 3.3 (SiC_4). TGA (1400 °C, 63% ceramic yield): 25−300 °C, Δm = 22%; 300−650 °C, Δm = 14%; 1150−1400 °C, Δm = 1%.

Scheme 1. Synthesis of Tris(hydridosilylethyl)boranes[21]

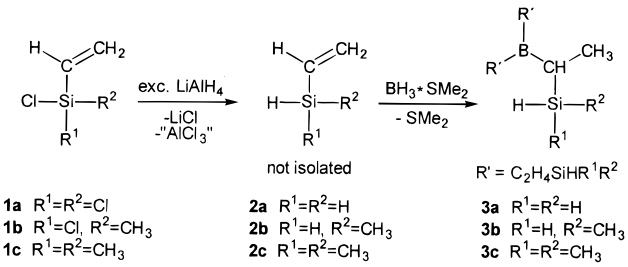

3. Results and Discussion

3.1. Synthesis. The synthesis of the starting compounds tris(hydridosilylethyl)boranes, $B(C_2H_4{-}SiH_3)_3$ (**3a**), $B[C_2H_4{-}Si(CH_3)H_2]_3$ (**3b**), and $B[C_2H_4{-}Si(CH_3)_2H]_3$ (**3c**), can be performed by different procedures.[21] The synthetic pathway used here starts from chlorovinylsilanes $(H_2C{=}CH)SiClR^1R^2$ (**1a**: $R^1 = R^2 =$ Cl; **1b**: $R^1 =$ Cl, $R^2 = CH_3$; **1c**: $R^1 = R^2 = CH_3$) and $LiAlH_4$. The respective hydridovinylsilanes $(H_2C{=}CH)SiHR^1R^2$ (**2a**: $R^1 = R^2 =$ H; **2b**: $R^1 =$ H, $R^2 = CH_3$; **2c**: $R^1 = R^2 = CH_3$) were reacted further with borane dimethyl sulfide in toluene solution. With respect to their difficult handling—hydridovinylsilanes can explode violently when exposed to air—these compounds where not isolated but reacted in situ according to Scheme 1.

The volatile parts of the reaction mixture that contains the vinylsilanes **2a**−**c**, solvent, byproducts, and excess $LiAlH_4$ were directly distilled into the $BH_3{\cdot}S(CH_3)_2$ solution. After purification by distillation, the tris(hydridosilylethyl)boranes $B(C_2H_4{-}SiHR^1R^2)_3$ ($C_2H_4 = CHCH_3$, CH_2CH_2; **3a**: $R^1 = R^2 =$ H; **3b**: $R^1 =$ H, $R^2 = CH_3$; **3c**: $R^1 = R^2 = CH_3$) were isolated as colorless liquids in quantitative yields according to the amount of borane dimethyl sulfide used. Caution: Compounds **2a**−**c** are extremely sensitive and can explode spontaneously in contact with air. Experimental details and full spectroscopic data are published elsewhere.[21]

The second component used for the synthesis of the title compounds was oligovinylsilazane (OVS, **4**). OVS was obtained by ammonolysis of vinyldichlorosilane, $(H_2C{=}CH)SiHCl_2$, according to a method described by Choong Kwet Yive and co-workers.[20] In this method, a mixture of cyclic silazanes was obtained in addition to oligosilazane chains. The molecular weight distribution of OVS depends on the solvent used and the reaction temperature applied.[20] Toluene was chosen here to get the highest average molecular weight OVS ($\bar{M}_w$ = 600 g/mol).

The synthesis of the Si−B−C−N precursors **5a**−**c** was performed according to Scheme 2 by a thermally induced hydrosilylation reaction of $B(C_2H_4{-}SiHR^1R^2)_3$ (**3a**−**c**) with OVS (**4**) in neat form without the use of a catalyst.

The starting compounds **3a**−**c** and OVS (**4**) were mixed at room temperature in a Schlenk tube and the resulting colorless reaction mixture was degassed in a vacuum. During heating of the mixtures to 120 °C within 2 h and then to 180−200 °C within 4−5 h, a remarkable viscosity increase was observed in the formation of the transparent, colorless glasslike solid. The determination of proper conditions for the hydrosilylation was performed when the reaction was moni-

Table 1. Calculated and Measured Elemental Composition [wt %, Scaled to 100%] for Compounds 5a−c and the Corresponding Formulas per Monomer Unit[a]

	5a		5b		5c	
polymer	calc.	meas.	calc.	meas.	calc.	meas.
Si	41.9	43.6	38.0	39.3	34.7	33.2
B	2.7	2.5	2.4	2.2	2.2	2.2
C	35.9	31.4	40.6	39.1	44.5	43.8
N	10.5	13.3	9.5	10.6	8.6	11.4
H	9.0	9.2	9.5	8.8	10.0	9.4
calc.	$Si_6BC_{12}N_3H_{36}$		$Si_6BC_{15}N_3H_{42}$		$Si_6BC_{18}N_3H_{48}$	
empirical	$Si_6B_{0.9}C_{10.1}N_{3.6}H_{35.3}$		$Si_6B_{0.9}C_{14}N_{3.3}H_{42.6}$		$Si_6BC_{18.8}N_{4.1}H_{47.4}$	

[a] Oxygen values are <1% and omitted.

Scheme 2. Synthesis of the Title Compounds 5a−c from Oligovinylsilazane (OVS, 4) and Tris(hydridosilylethyl)boranes 3a−c and OVS (4)

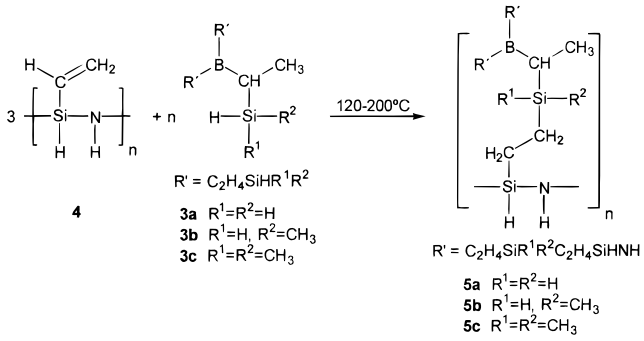

Scheme 3. Hydroboration of Vinylsilanes Is Not Regioselective (Schematical Representation); Depending on the Nature of Substituents R^1 and R^2, Different α:β Product Ratios Are Observed[22,24]

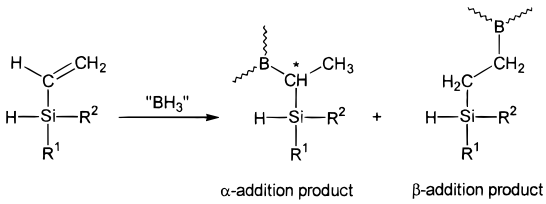

tored with IR spectroscopy. Heat treatment was continued until the ν(C═C) stretching at 1598 cm^{-1} and the ν(═C−H) vibrations at ∼3050 cm^{-1} of OVS could no longer be detected. In the case of the highly reactive tris(trihydridosilylethyl)borane **3a**, a heat treatment above 130 °C was not necessary. The reaction mixtures of the less reactive methyl-substituted tris(hydridosilylethyl)boranes **3b** or **3c** with OVS were heated to 200 °C and held for 18 h (**3b**) or 24 h (**3c**). After the reaction mixtures underwent additional heating in a vacuum (150−160 °C, 10^{-3} mbar), milling, and sieving, the products were obtained as colorless powders, each in 100% yield. The polymers do not melt without decomposition and they are insoluble in any common organic solvent. Because of the very simple, well-controllable synthetic procedure and the lack of solvent, the scale applied for the precursor synthesis can be extended to any desired level.

3.2. Precursor Characterization. Chemical composition and structure of compounds **5a−c** were investigated by microanalysis, solid-state NMR and IR spectroscopy. Because of the insolubility of the title compounds, neither high-resolution NMR investigations in solution nor molecular weight determination could be performed.

Prior to their characterization, the cross-linked glass-like polymers were pulverized by ball mill grinding (ZrO_2) and homogenized by sieving through 80-μm mesh-size stainless steel sieves within a glovebox. Table 1 gives a comparison of the calculated and the measured elemental composition for the powders of **5a−c**, scaled to 100%, and the corresponding formulas per monomer unit (oxygen values were determined to be <1% and omitted).

The element ratios in the empirical formulas per monomer unit do not show major deviations from the expected calculated compositions. However, because of its low boiling point, **3a** in part evaporates during the cross-linking. In the colder zone of the reaction vessel it condenses and refluxes. This results in a slight fluctuation in the homogeneity of **5a**, resulting in a low determination of the carbon content.

It is difficult to structurally characterize the title compounds because of the limitation of applicable spectroscopic methods, that is, because high-resolution NMR spectroscopy cannot be applied as a result of the poor solubility of the title compounds. To unequivocally assign the detailed structure of compounds **5a−c** from spectroscopic data, it is necessary to first discuss a number of conceivable single-reaction steps. Initially, it has to be considered that the hydroboration of vinylsilanes **2a−c** for the synthesis of the starting compounds **3a−c** is not regioselective. Boron addition onto the C═C units in both the α- and β-positions of the silicon atoms is observed (Scheme 3).[21,23]

The α:β ratio in the case of the synthesis of compounds **3**, which was determined by high-resolution NMR in solution, is at 3.3:1 for **3a** and 1.7:1 for **3b**, whereas in the case of the dimethyl-substituted derivative **3c** the α:β ratio decreases to 0.9:1. This tendency can be explained with steric and electronic effects. Because of both, α- and β-hydroboration, CH_3, CH_2, and CH units are formed. Moreover, α-boron addition causes chiral centers at the silicon-bonded carbon atom, which complicates the spectra because of the formation of ααα- and ααβ- diastereotopes. For example, the aliphatic area of the ^{1}H NMR spectrum of **3b**, dissolved in C_6D_6, is depicted in Figure 1 to illustrate the complexity of the NMR spectra of the starting compounds **3a−c**.

As shown in Figure 1, the appearance of different regioisomers and diastereomers causes sets of resonance signals that remarkably overlap. For the silicon-bonded methyl group a set of seven resonance signals is found in the −0.07 to 0.05 ppm range. The coupling with SiH_2

(23) Jones, P. R.; Myers, J. K. *J. Organomet. Chem.* **1972**, *34*, C9.

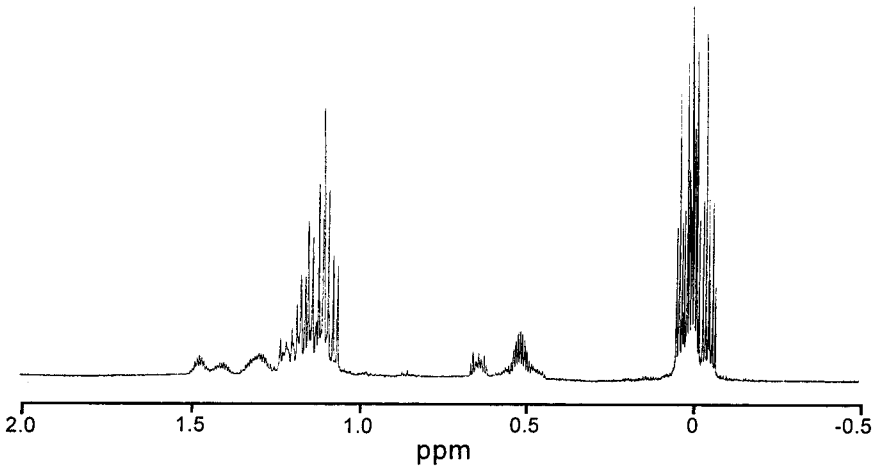

Figure 1. ^{1}H NMR (500.13 MHz, C_6D_6) of the aliphatic area of $B[C_2H_4-Si(CH_3)H_2]_3$ (**3b**; C_2H_4 = $CHCH_3$, CH_2CH_2).

Scheme 4. Possible Isomers Caused by Thermally Induced Hydrosilylation of Oligovinylsilazane (OVS, 4) with Tris(hydridosilylethyl)boranes 3a−c

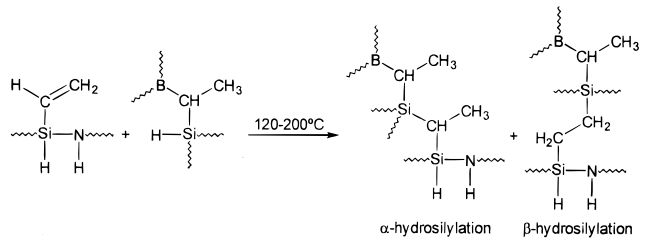

protons ($^3J_{H-H} \approx 4.1-4.2$ Hz) splits them into triplets. At 0.46−0.55 and at 0.62−0.66, $SiCH_2$ (caused by β-boron addition) resonance signals are found. They appear as multiplets because of their coupling with SiH_2 and with BCH_2 protons, which show resonance at ≈1.15−1.23 ppm. The $CHCH_3$ protons and the $CHCH_3$ protons, which are caused by α-boron addition to the olefin unit, are found as broad peaks at 1.26−1.49 ppm and as doublets with $^3J_{H-H} \approx 7$ Hz at ≈1.04−1.16 ppm, respectively. For detailed investigations of the structure of compounds **3a−c**, see ref 21.

Hydrosilylation, as represented in Scheme 4 can also occur in the α- and β-positions to the silicon centers, even though head-to-tail addition is favored.[24]

The regioselectivity of the hydrosilylation in the synthesis of **5a−c** is more difficult to investigate than that of the hydroboration of the vinylsilanes discussed above. The reasons are as follows:

(1) The highly cross-linked precursors cannot be examined by high-resolution NMR spectroscopy in solution.

(2) CH, CH_2, and CH_3 resonance signals of the conceivable $Si-CH(CH_3)-Si$ (α-hydrosilylation product) and $Si-CH_2-CH_2-Si$ (β-addition product) moieties overlap with those of the $Si-CH(CH_3)-B$ and the $Si-CH_2-CH_2-B$ units, which are present in the starting compounds **3a−c** (compare Schemes 3 and 4).

(3) A quantitative determination of the distribution of the regioisomers built because of the thermally induced hydrosilylation step by solid-state NMR spectroscopy fails as a result of significantly broadened resonance signals, which lack any fine structure.

Scheme 5. Cross-linking of Oligovinylsilazane (OVS, 4) and Tris(hydridosilylethyl)boranes 3a−c by Dehydrogenative Si−N Bond Formation

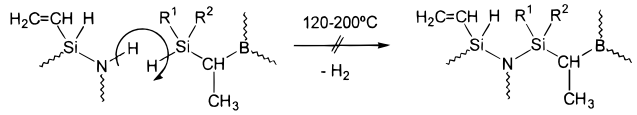

In addition, there is a number of possible side reactions that have to be taken into account, for example, the cross-linking of the starting compound oligovinylsilazane (OVS, **4**). This can occur by either hydrosilylation, olefin polymerization, or *trans*-amination as published by Chong Kwet-Yive and co-workers.[20] In the first case, the $SiC(sp^2)HN_2$ silicon environment in OVS would be transformed into a $SiC(sp^3)_2N_2$ site, while cross-linking due to the desired tris(hydridosilylethyl)-borane addition would result in a $SiC(sp^3)HN_2$ environment. *Trans*-amination of OVS in the synthesis of **5a−c**, which would be accompanied by the loss of ammonia, can be excluded if the results of the elemental analysis are considered. Cross-linking of OVS by olefin polymerization would cause the formation of aliphatic carbon sites besides the transformation of $SiC(sp^2)HN_2$ into $SiC(sp^3)HN_2$ silicon sites. Moreover, residual unreacted Si−H groups of the starting compounds **3a−c** would be expected. Even though steric aspects make it less likely, "double" hydrosilylation reactions of $B(C_2H_4-SiRH_2)_3$ (**3a** R = H; **3b** R = CH) are also possible. Hereby, $Si(sp^3)_3H$ sites (hydrosilylation of OVS with **3a**) or $Si(sp^3)_4$ sites (hydrosilylation of OVS with **3b**) should be observed.

Considering matching hydrogen values found by elemental analysis (compare Table 1) combined with quantitative polymer yields and the lack of gases forming during the cross-linking, dehydrogenative Si−N coupling, as schematically represented in Scheme 5, can be excluded. This is a crucial fact because the loss of hydrogen during the cross-linking step would cause bubbles, which would disqualify the precursors as matrix materials for fiber-reinforced composites.

However, by using solid-state NMR techniques, valuable information about the molecular structures of **5a−c** is available. Figure 2 shows the ^{1}H solid-state NMR spectra of the title compounds **5a−c** and OVS (**4**). The latter was heat-treated under the same conditions used

(24) Musolf, M. C.; Speier, J. L. *J. Org. Chem.* **1964**, *29*, 2519.

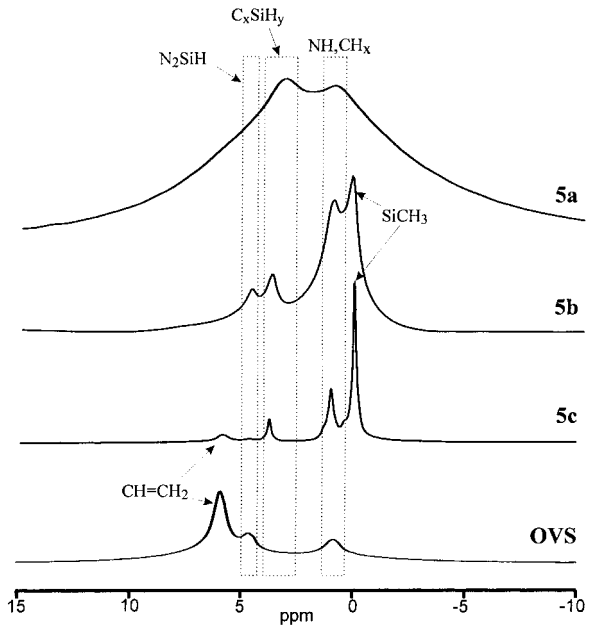

Figure 2. ^{1}H solid-state NMR (300.13 MHz) spectra of OVS (**4**) and compounds **5a**−**c**.

for the synthesis of **5a**−**c**. The dotted frames give chemical shift ranges of different expected functional groups. In the 0.3−1.4 ppm range N*H*, C*H*, CH_2, and CH_3 resonance signals are observed. In the 2.6−3.8 ppm range various C_xSiH_{4-x} resonances are found while "silazane" N_2SiH resonance signals are found around 4.5 ppm.

Even though the spectrum of **5a** shows extremely broadened lines, it can be assumed that it exhibits the expected N*H*, C*H*, CH_2, CH_3, C_xSiH_{4-x}, and N_2SiH structural entities. Resonance signals of vinyl protons that would point to incomplete hydrosilylation are not present. Similar findings are made in the spectrum of **5b**, which has higher resolution. Besides the expected signals centered at 0.9, 3.6, and 4.4 ppm that were already discussed for **5a**, this plot shows an additional resonance signal at 0 ppm. This can be associated with a silicon-bonded methyl group that is already present in the starting compound $B[C_2H_4-Si(CH_3)H_2]_3$ (**3b**). This Si−CH_3 signal is dominant in the ^{1}H NMR spectrum of **5c** because of the presence of two methyl groups in the starting compound $B[C_2H_4-Si(CH_3)_2H]_3$ (**3c**). Moreover, there is an unexpected C_3SiH resonance signal observed at 3.7 ppm. In combination with a vinyl resonance signal of minor intensity around 5.8 ppm, it can be assumed that the hydrosilylation in the reaction of OVS with **3c** did not occur quantitatively, possibly because of the steric demanding $Si(CH_3)_2H$ entities.

The observations made in the proton NMR spectra are nicely reflected in the ^{13}C NMR spectra of the title compounds (Figure 3).

The hydrosilylation of the vinyl units in OVS (**4**) causes a high field shift of the vinyl carbons from 135 and 139 ppm in the starting compounds to ≈10−25 ppm in the final products. As denoted above, proper differentiation of Si−C_2H_4−B and Si−C_2H_4−Si units (C_2H_4 = $CHCH_3$, CH_2CH_2) is not possible. Compounds **5a**−**c** each show broad and overlapping C*H*, CH_2, and C*H*CH_3 signals in the 10−28 ppm range. Nevertheless, it is obvious that the tendency for α-addition reactions (hydroboration and/or hydrosilylation) increases in the following manner: **5c** < **5b** < **5a**. This can be concluded from the increasing C*H*CH_3 signal intensity. The ^{13}C NMR spectra of **5b** and **5c** possess additional resonance

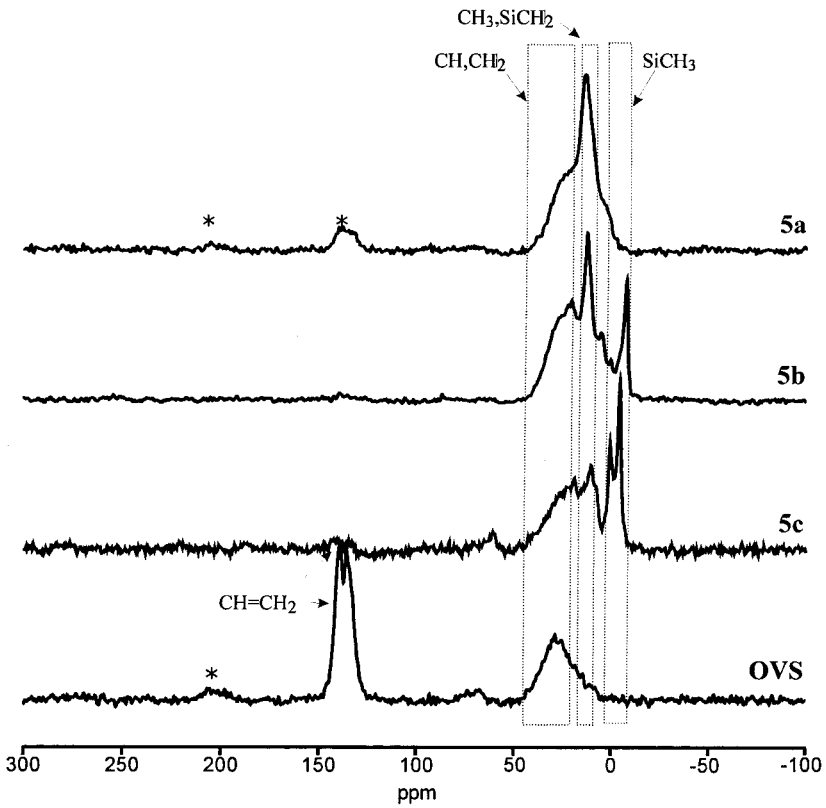

Figure 3. ^{13}C CP-MAS NMR (75.47 MHz) spectra of OVS (**4**) and compounds **5a**−**c**. Spinning sidebands are marked with an asterisk.

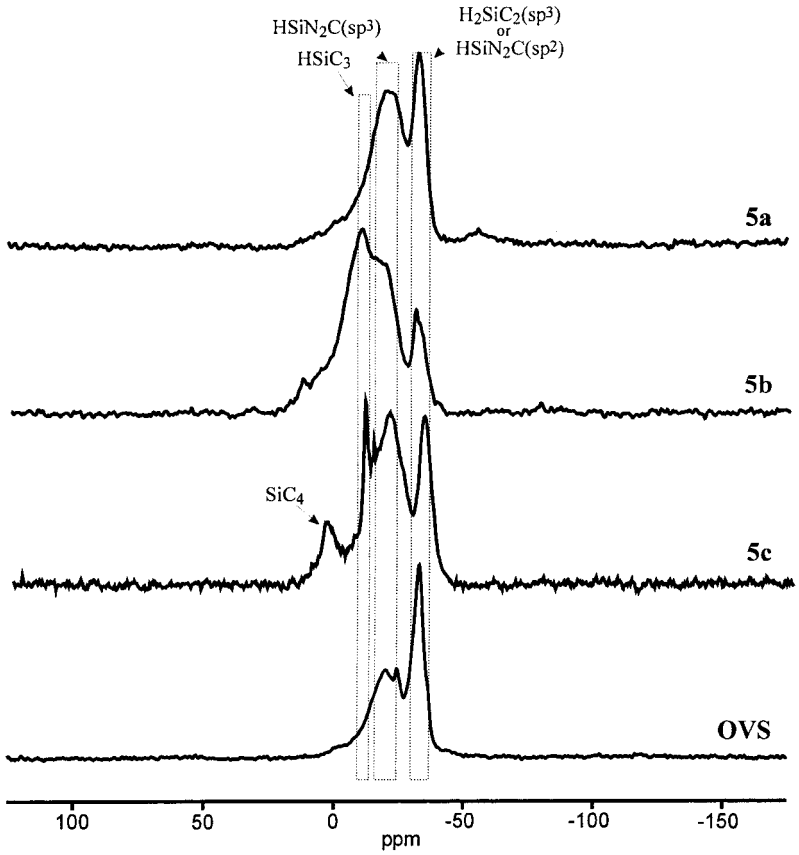

Figure 4. ^{29}Si CP-MAS NMR (59.60 MHz) spectra of OVS (**4**) and compounds **5a**−**c**.

signals at −6.5 ppm (**5b**) and 1.2 ppm as well as −3.5 ppm (**5c**), which can be attributed to the C_2SiHCH_3 and $C_2Si(CH_3)_2$ sites. The signal at −3.5 ppm in the spectrum of **5c** corresponds to a C_2SiHCH_3 site. In accordance with the ^{1}H NMR spectrum in Figure 2 the hydrosilylation in this particular reaction was incomplete. As a consequence, vinyl resonance signals of very low intensity are observed at 133 and 139 ppm. Pure OVS, in contrast, delivers a polymer that contains a remarkable amount of vinyl groups in addition to aliphatic carbons (CH_2−CH_2), which are built by olefin polymerization. As expected, in this case, $CHCH_3$ signals are not observed.

These conclusions are supported by the ^{29}Si NMR spectrum (Figure 4) of OVS, which shows a $HSiN_2C(sp^2)$ resonance signal at −33 ppm aside from a broad $HSiN_2C(sp^3)$ resonance at −19 ppm. $SiN_2C(sp^3)_2$ sites at around −5 ppm due to hydrosilylation are not observed.

This is an important fact because OVS "self-hydrosilylation" can be excluded in all polymers. While the ^{29}Si NMR of **5a** shows the expected $H_2SiC(sp^3)_2$ sites at −32 ppm besides $HSiN_2C(sp^3)$ at −20 ppm the spectra of **5b** and **5c** are complex and more difficult to discuss. First of all, the spectra of the latter compounds possess the required $HSiN_2C(sp^3)$ sites representing the silazane skeletons at around −18 ppm as well as $HSiC(sp^3)_3$ (**5b**) and $SiC(sp^3)_4$ (**5c**) at −11.5 and 3.3 ppm, respectively. Surprisingly, a resonance signal at −31.4 ppm is observed in the spectrum of **5b** that is attributed to $H_2SiC(sp^3)_2$. $HSiN_2C(sp^2)$ sites, pointing to residual OVS units, (H_2C=CH)SiH−NH, can be excluded, reflecting on the proton and carbon NMR of **5b**. A possible explanation for the appearance of $H_2SiC(sp^3)_2$ is thus to consider double hydrosilylation of the C_2H_4−$Si(CH_3)H_2$ units in the starting compound **3b** with the formation of $SiC(sp^3)_4$ units. The respective sites at ≈3 ppm are observed as a shoulder of the dominant $HSiC(sp^3)_3$ resonance that corresponds to the expected main product. Inadequate hydrosilylation for the synthesis of **5c**, as already discussed in the ^{1}H and ^{13}C NMR spectra, can also be concluded from the silicon NMR of this compound. This is reflected by the presence of $HSiN_2C(sp^2)$ sites (−34.8 ppm) due to remaining vinyl units as well as by $HSiC(sp^3)_3$ moieties found at −11.9 ppm that correspond to residual C_2H_4−$Si(CH_3)_2H$ units of **3c**.

The infrared spectra of the polymers **5a**−**c** clearly show the typical absorption signals of the expected groupings: ν (N−H) are found at ≈3400 cm^{-1} as broad peaks, and three sharp peaks due to ν (C−H) are observed between 3049 and 2869 cm^{-1}. Other characteristic absorption signals are ν (Si−H), which are found as very sharp peaks at ≈2144 cm^{-1} for **5a** and 2130 cm^{-1} for **5b** and **5c**, δ (CH_2) at around 1450 cm^{-1}, and ν (C−C) at 1162−1168 cm^{-1}. Very weak C=C vibrations in the IR spectrum of **5c** due to incomplete cross-linking are observed at 1595 cm^{-1}. The corresponding =C−H vibrations are observed at 3049 cm^{-1}. For further details see the Experimental Section. The spectroscopic data and characterization of **5b** are also described in ref 25.

3.3. Ceramic Materials. Ceramic materials **6a**−**c** were obtained by thermolysis of compounds **5a**−**c**. The precursors were heated in Al_2O_3 Schlenk tubes under an argon atmosphere to 1400 °C with a heating rate of

(25) Bill, J. et al. *Appl. Organomet. Chem*. submitted.

Table 2. Elemental Composition of Ceramic Materials 6a−c [wt %, at. %, Scaled to 100%] and Phase Fractions [mol % of Atoms] Calculated by the Calphad Method[26] [a]

	6a		6b		6c	
	wt %	at %	wt %	at %	wt %	at %
Si	48.4	29.2	46.3	27.4	44.1	26.0
B	3.4	5.4	3.6	5.6	4.0	6.1
C	34.3	48.6	37.8	52.4	32.5	44.9
N	13.9	16.8	12.3	14.6	19.4	23.0
ceramic	$Si_6B_{1.1}C_{10}N_{3.4}$		$Si_6B_{1.2}C_{11.5}N_{3.2}$		$Si_6B_{1.4}C_{10.3}N_{5.3}$	
(polymer)	$(Si_6B_{0.9}C_{10.1}N_{3.6}H_{35.3})$		$(Si_6B_{0.9}C_{14}N_{3.3}H_{42.6})$		$(Si_6BC_{18.8}N_{4.1}H_{47.4})$	
BN	10.8		11.2		12.2	
Si_3N_4	19.9		15.7		29.6	
SiC	41.3		41.3		26.6	
C	28.0		31.8		31.6	

[a] Oxygen is <1%.

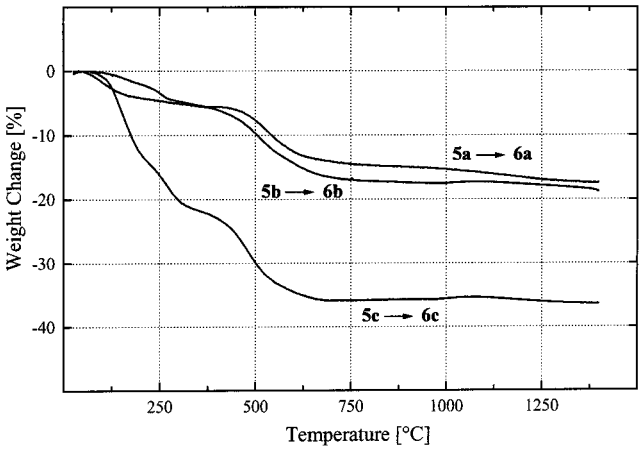

Figure 5. TGA in alumina crucibles of the polymer-to-ceramic conversion of **5a**−**c** → **6a**−**c**; heating rate: 2 °C/min; atmosphere: flowing argon.

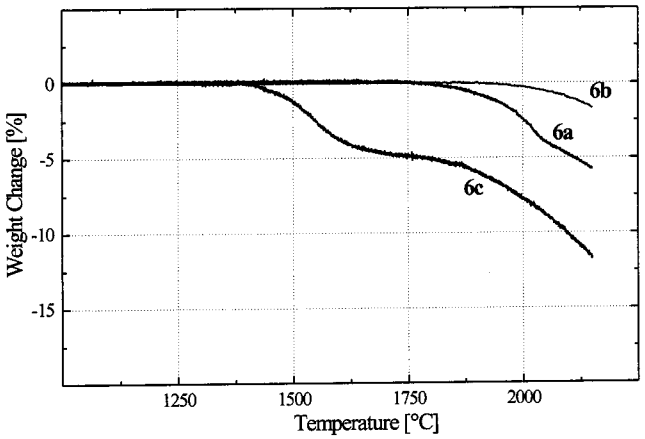

Figure 6. High-temperature TGA of ceramics **6a**−**c**. Heating rate: T < 1400 °C, 5 °C/min; T > 1400 °C, 2 °C/min; argon atmosphere, carbon crucibles.

1 °C/min. To ensure complete ceramization, the precursors were held for 2 h at 1400 °C. The as-obtained ceramics are black solids, which are X-ray amorphous (compare Figure 8). Their chemical composition was determined by elemental analysis and is given in Table 2.

The thermal conversion of preceramic polymers into ceramic materials (thermolysis) is accompanied by the formation of gaseous byproducts. Consequently, a mass loss during the polymer-to-ceramic conversion occurs. The ceramic yields for the conversion of **5a**−**c** into the ceramics **6a**−**c** were determined using TGA (Figure 5).

The polymers possess very comparable ceramization progressions, marked by a two-step decomposition. The first step takes place in the 200−300 °C range, whereas the second step occurs between 400 and 600 °C. There is an additional mass loss of 1%−2% observed in each TGA plot in the 1100−1400 °C range, which is caused by hydrogen evaporation. Because of the high cross-linking of the polymers **5a** and **5b**, depolymerization during thermolysis is not observed. As a consequence, their ceramic yields are high: 83% for **5a** and 82% for **5b**. In comparison, the ceramic yield of **5c** is only 64%, which is probably a consequence of insufficient cross-linking, as already pointed out in the former section. Recently, we showed that the nature of the silicon-bonded substituents also plays an important role regarding ceramic yields.[12] While low-weight substituents and/or reactive groups are prerequisites for high ceramic yields, alkyl moieties cause significant loss; during heat treatment they split off in radical reactions as alkanes or alkenes. This is probably the second reason for the more pronounced mass loss of **5c** as compared to that of **5a** or **5b**.

The high-temperature stability of ceramics **6a**−**c** in an inert gas atmosphere over a temperature range of 25−2150 °C was determined by high-temperature thermogravimetric analysis in argon (HT-TGA, Figure 6) and by X-ray diffraction (XRD) of annealed ceramic samples (Figure 8) in nitrogen and theoretically supported by thermodynamic calculations using the CALPHAD method (calculation of phase diagrams).[26]

A comparison of the HT-TGA of ceramics **6a**−**c** shown in Figure 6 demonstrates significant differences in thermal stability. While the **6b** material starts to decompose around 2000 °C, the **6a** ceramic decomposes around 1850 °C. The ceramic obtained from **5c** is the least stable material and decomposes at ≈1450 °C. This value is typical for the decomposition of ternary Si−C−N ceramics that contain free carbon[27] and mirrors thermodynamic calculations carried out for several precursor-derived Si−B−C−N ceramics composed of silicon nitride aside from free carbon.[28] In the following

(26) (a) Kasper, B. Ph.D. Thesis, Universität Stuttgart, Germany, 1996 (in German). (b) Seifert, H. J.; Aldinger, F. *Z. Metallkd.* **1996**, *87*, 841. (c) Seifert, H. J.; Aldinger, F. In *Grain Boundary Dynamics of Precursor-Derived Ceramics*; Bill, J., Wakai, F., Aldinger, F., Eds.; Wiley-VCH: Weinheim, 1999; p 165.

(27) (a) Mocaer, D.; Pailler, R.; Naslain, R.; Richard, C.; Pillot, J. P.; Dunogués, J.; Gerardin, C.; Taulelle, F. *J. Mater. Sci.* **1993**, *28*, 2615. (b) Kleebe, H.-J.; Suttor, D.; Müller, H.; Ziegler, G. *J. Am. Ceram. Soc.* **1998**, *81*, 2971. (c) Bill, J.; Seitz, J.; Thurn, G.; Dürr, J.; Canel, J.; Janos, B.; Jalowiecki, A.; Sauter, D.; Schempp, S.; Lamparter, P.; Mayer, J.; Aldinger, F. *Phys. Stat. Sol.* **1998**, *166*, 269.

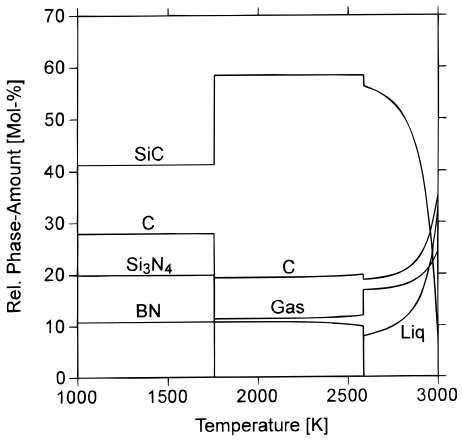

Figure 7. Calculated phase fraction diagram ($p_{tot} = 1$ bar) of **6a** material (Si, 29.2; B, 5.4; C, 48.6; N, 16.8 [at. %]). Reaction of Si_3N_4 and graphite at 1484 °C (1757 K) results in the formation of SiC and N_2 (Gas).

the calculated phase fraction diagram of the **6a** ceramic, which is depicted in Figure 7, is discussed in more detail.

According to these calculations, which are listed in Table 2 and graphically represented in Figure 7, **6a** is composed of 10.8 mol % of BN, 19.9 mol % of Si_3N_4, 41.3 mol % of SiC, and 28 at. % of graphite. At 1484 °C (1757 K) Si_3N_4 reacts with carbon under the formation of SiC and gaseous nitrogen. The phase amount of SiC increases to 58.4 mol % whereas the amount of graphite decreases by 8.5 to 19.5 at. %. Because of the formation of N_2 (gas), the sample weight decreases by 9.4 mass %. Similar observations are made for **6b** and **6c**. Both materials should decompose at 1484 °C with the formation of gaseous nitrogen. A conclusive description for the unexpected thermal stability of Si−B−C−N ceramics was published recently.[12] Most likely, a turbostratic B−C−N phase that forms inhibits diffusion processes and decreases the activity of free carbon.[29] Accordingly, the reaction of carbon with silicon nitride does not take place. Another important prerequisite for obtaining high-temperature stable materials is that the amount of silicon nitride does not exceed a certain value. Recent investigations showed that this value is at ≈30 mol %.[12,30] The lower thermal stability of **6c** compared to that of **6a** and **6b** is thus most likely due to its higher Si_3N_4 amount at 29.6 mol % compared to that at 19.9 or 15.7 mol % Si_3N_4, respectively.

XRD investigations of annealed ceramic samples as depicted in Figure 8 for **6a** ceramic material proved the formation of silicon nitride and silicon carbide crystalline phases. As-obtained ceramic material was annealed in carbon crucibles at various temperatures in the 1500−2000 °C range.

After thermolysis, the **6a** ceramic obtained is fully amorphous. With increasing temperature the amorphous material demixes. At 1550 °C broad reflections at $2\theta = 36°$ and 61° appear, suggesting the formation of nanocrystalline silicon carbide. At 1750 °C these reflections sharpen because of ongoing silicon carbide

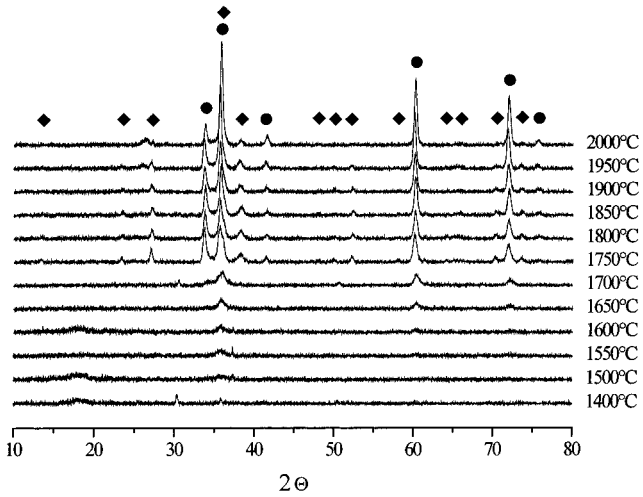

Figure 8. XRD patterns of **6a** ceramic material annealed at 1400 and 1500−2000 °C (50 °C steps, 1 bar nitrogen) each for 3 h (●, α-SiC; ◆, β-Si_3N_4).

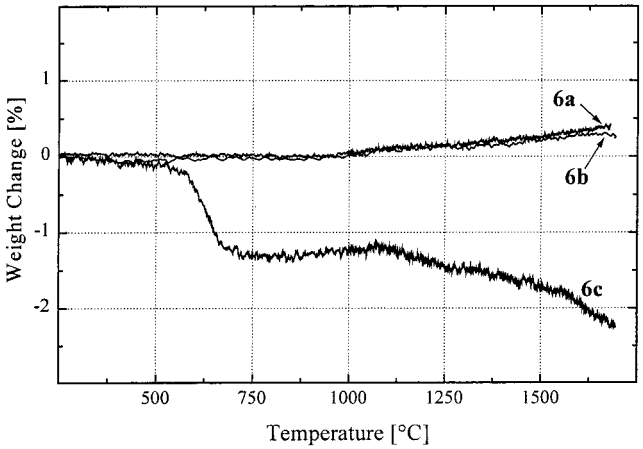

Figure 9. High-temperature TGA of ceramics **6a**−**c** in air. Heating rate: T < 1000 °C, 10 °C/min; T > 1000 °C, 5 °C/min; alumina crucibles.

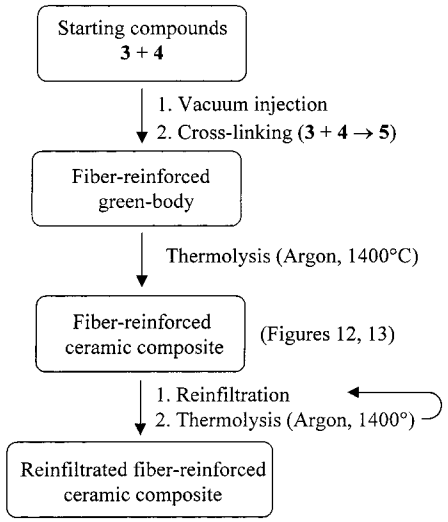

Figure 10. Flow diagram for the preparation of fiber-reinforced ceramics from tris(hydridosilylethyl)boranes (**3**) and oligovinylsilazane (OVS, **4**) by RTM.

(28) (a) Seifert, H. J.; Lukas, H.-L.; Aldinger, F. *Ber. Bunsen-Ges. Phys. Chem.* **1998**, *102*, 1309. (b) Seifert, H. J.; Peng, J.; Aldinger, F. In *Proceedings Werkstoffwoche '98*; Heinrich, J., Ziegler, G., Hermel, W., Riedel, H., Eds.; Wiley-VCH: Weinheim, 1999; p 165. (c) Peng, J.; Seifert, H. J.; Aldinger, F. *Euromat 99*, submitted.

(29) (a) Jalowiecki, A.; Bill, J.; Aldinger, F.; Mayer, J. *Composites* **1996**, *27A*, 717. (b) Jalowiecki, A. Ph.D. Thesis, Universität Stuttgart, Germany, 1997 (in German).

(30) Weinmann, M.; Katz, S.; Berger, F.; Kaiser, G.; Müller, K.; Aldinger, F. *Appl. Organomet. Chem.*, submitted.

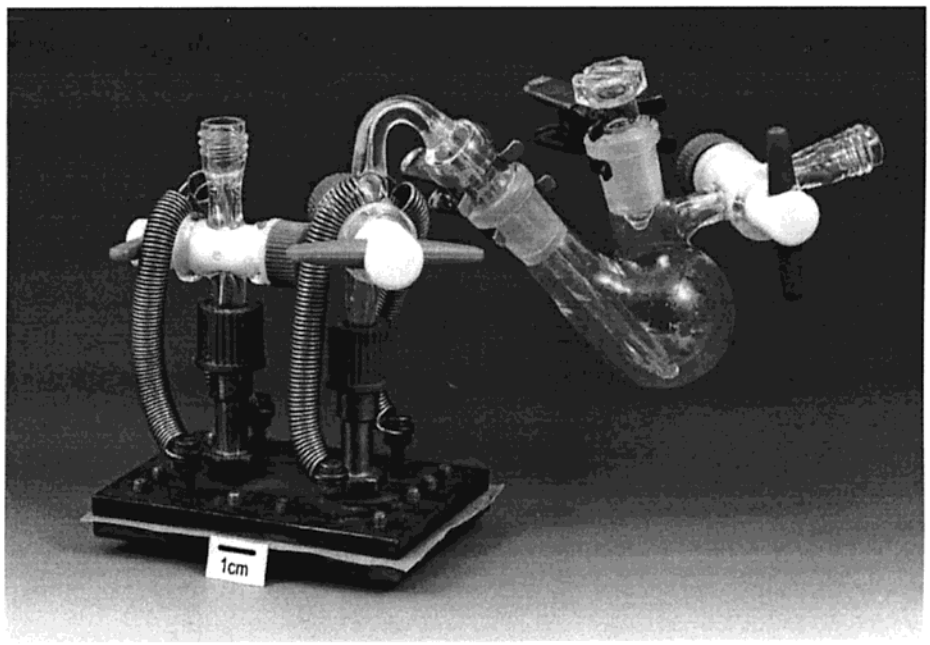

Figure 11. RTM vacuum injection equipment consisting of a brass mold that contains fiber fabrics or a three-dimensional weave and a Schlenk flask that serves as a reservoir for the precursor mixture.

crystallization. Crystallization of β-silicon nitride is also observed at this temperature. Even though the intensities of the silicon nitride reflections decrease with increasing temperature, they persist after the ceramic is annealed to 2000 °C. This is surprising because under the present conditions applied silicon nitride decomposition into the elements should occur at around 1850 °C.[28] Finally, a broad reflection at $2\theta = 26.3°$ evolving at 1950 °C can be assigned to crystalline graphite.

Preliminary investigations of the resistance of **6a−c** toward oxidation and hydrolysis at elevated temperature were performed by the recording of high-temperature TGA in air up to 1700 °C. The results that are shown in Figure 9 point out that only a negligible mass gain of roughly 0.3% is observed in the case of the **6a** and **6b** materials. This effect is most likely due to a passive oxidation of the ceramics that is accompanied by the formation of a Si(C)O layer that prevents the matrix from further oxidation or hydrolysis. Similar findings were described recently for a couple of other Si−B−C−N materials.[12] In contrast, a mass loss of 1.3% is observed in the TGA of **6c** already at 600 °C. Additional mass loss at 1450 °C in the TGA of **6c** points to its beginning decomposition that was also observed in the high-temperature TGA in argon (compare Figure 6).

3.4. Preparation of Fiber−Matrix Composites. First orienting experiments have proven the applicability of the title compounds in the resin-transfer-molding (RTM) process. Torayca carbon woven fabrics were used as reinforcement and **5b** as the matrix material. Some particular requirements that the preceramic material sufficiently fulfills are as follows: (1) low viscosity (fluidity) of the starting compounds to allow sufficient penetration; (2) adequate vapor pressure (resin transfer is performed by vacuum injection); (3) appropriate chemistry (no solvents or byproducts) and controllable reactivity during cross-linking; (4) high thermolysis conversion yields/low shrinkage during thermolysis.

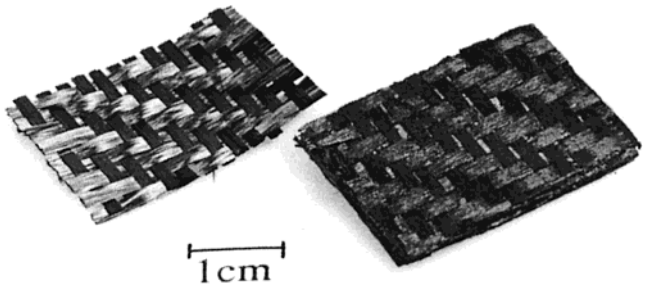

Figure 12. Fiber fabrics before (left) and after RTM and thermolysis (right). The fiber-reinforced ceramic substrate consists of eight layers of fiber fabrics and was not re-infiltrated.

The single steps of the RTM process, as it was performed for the preparation of the ceramic fiber−matrix composites, is shown schematically in Figure 10.

The particular sensitivity of the starting compounds **3a−c** and OVS (**4**) toward oxygen and moisture made it necessary to develop the equipment shown in Figure 11 to avoid precursor contact with air. It consists of a Schlenk flask, which serves as a reservoir for the precursor mixture, and a brass mold, which contains fiber fabrics or alternatively three-dimensional weave. Both parts are linked via an interconnection glass tube. The valves attached allow separate evacuation of the two main parts. Initially, the brass mold is filled with the fiber material and the whole system thoroughly evacuated. The central valve is closed and the Schlenk flask flooded with inert gas. The reaction mixture is introduced and the Schlenk flask evacuated again. After the central valve is opened, the precursor mixture is injected into the brass mold by slow introduction of argon through the valve attached to the Schlenk tube. After injection, the central valve is closed again and the brass mold heated within an oil bath to cross-link the precursors (Figure 10, step 1). The fiber-reinforced green body is removed from the brass mold within a glovebox. Subsequent thermolysis of the bulk part in Al_2O_3

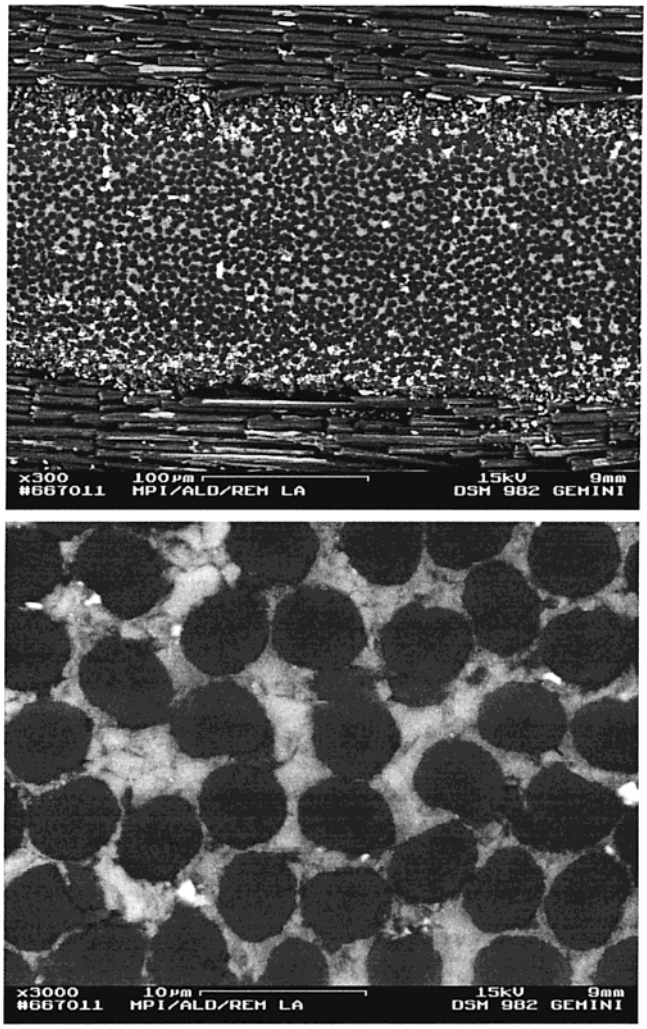

Figure 13. Scanning electron micrographs of a cross-section of the fiber-reinforced **6b** ceramic shown in Figure 11 at 300× magnification (top) and 3000× magnification (below). In the upper part of the top image a fiber bundle (dark gray) parallel to the view is seen, followed by a fiber bundle with perpendicular orientation in the center image. The image at 3000× magnification shows fibers well embedded by the Si−B−C−N matrix. White spots in both images are due to impurities caused by the preparation of the samples.

Schlenk tubes in an argon atmosphere up to 1400 °C (Figure 10, step 3) then delivers the fiber-reinforced ceramic composite shown in Figure 12.

Scanning electron micrographs of a polished cross-section of this fiber-reinforced specimen are depicted in Figure 13 at 300× magnification (top) and 3000× magnification (below). In the image at 300× magnification it is seen that the fibers are oriented with their long axis bundled alternatively parallel and perpendicular to the viewer. Elongated dark gray regions correspond to the parallel view of the long axis of the carbon fibers and the dark gray dots correspond to the end-on view of the fibers. The fibers are bundled in layers that are ≈170-μm thick. The Si−B−C−N matrix appears as a light gray region filling the space between the fibers. White spots in both images are due to impurities caused by the preparation (polishing) of the samples. The image at 3000× magnification suggests that the carbon fibers are homogeneously wrapped by the Si−B−C−N matrix. However, the matrix is not fully dense; it is composed of ceramic grains with sizes ranging from <1 to 3 μm.

The porosity of the fiber-reinforced **6b** ceramic part was 25%, as determined by mercury pressure porosimetry, whereas the porosity of pure **6b** was 6%. The most likely reasons for this difference are insufficient resin transfer and different matrix shrinkage in the fiber-reinforced and the fiber-free materials during thermolysis. Excessive porosity could be decreased to <15% by repetition of the injection and thermolysis procedures three times (Figure 10, step 3).

Measurement of the mechanical properties, such as creep, bend strength, shear strength, and fracture toughness of the fiber-reinforced materials, remains for future perspectives.

Conclusions

Thermally induced hydrosilylation of oligovinylsilazane with tris(hydridosilylethyl)boranes, $B[C_2H_4-Si(CH_3)_nH_{3-n}]_3$ ($n = 0 - 2$), is a suitable synthetic procedure for the preparation of precursors for high-temperature stable fiber-reinforced Si−B−C−N ceramics. Polymer synthesis occurs quantitatively without the requirement of solvents or catalysts and without the formation of any byproducts. The physical−chemical properties of the starting compounds and the straightforward synthetic procedure—the starting compounds are simply mixed and reacted at moderate temperature—allow the preparation of fiber-reinforced Si−B−C−N green parts using the RTM process. Thermolysis of the green parts delivers fiber-reinforced ceramics with an amorphous Si−B−C−N matrix. Depending on the starting compounds used, the materials are thermally stable in an inert gas atmosphere up to 2000 °C. Transformation of the amorphous materials into crystalline SiC/Si_3N_4 composites can be performed by additional heat treatment in the 1600−1750 °C range. Because these first orienting results are very promising, additional detailed investigations will be performed soon. The main focus of these studies will be to increase the bulk density and to control the fiber−matrix bonding and debonding behavior.

Acknowledgment. The authors warmly thank Horst Kummer for high-temperature TGA measurements and Martina Thomas for assistance in XRD investigations. Jianqiang Peng and Dr. Hans Jürgen Seifert are acknowledged for carrying out thermodynamic calculations. Dr. Joachim Bill is acknowledged for helpful discussions and Dr. Judy Schneider is acknowledged for her help in the preparation of the manuscript. This study was financially supported by the Keramikverbund Karlsruhe-Stuttgart (KKS), Deutsche Forschungsgemeinschaft (DFG), and Japan Science and Technology Corporation (JST).

CM001031W